RSC Advances

PAPER

View Article Online
View Journal | View Issue

Cite this: *RSC Adv.*, 2016, **6**, 9884

Cation-sensitive compartmentalization in metallacarborane containing polymer nanoparticles†

Vladimír Ďorďovič,[a] Mariusz Uchman,[a] Mehedi Reza,[b] Janne Ruokolainen,[b] Alexander Zhigunov,[c] Olexandr I. Ivankov[de] and Pavel Matějíček*[a]

Received 23rd December 2015
Accepted 13th January 2016

DOI: 10.1039/c5ra27588a

www.rsc.org/advances

Alkaline cations (Li^+, Na^+ and K^+) are introduced as agents suitable to control compartmentalization in metallacarborane-rich nanoparticles of double-hydrophilic block copolymer poly(ethylene oxide)-*block*-poly(2-alkyloxazoline), PEO–POX. Interaction of the metallacarborane (cobalt bis(dicarbollide) anion) with PEO–POX is based mainly on dihydrogen bonding between metallacarborane boron clusters and the polymer backbone resulting in compact nanoparticles. However, the cations are a crucial factor as to whether interaction with PEO or POX segments is preferred. Changes in the bulk concentration of alkaline cations can thus provoke changes in the inner structure of polymeric nanoparticles, which is accompanied by exchange of boron clusters and alkaline cations like Li^+. Because of the biomedical importance of metallacarboranes, their conjugates and also lithium salts, the hybrid nanoparticles can act as stimuli-responsive systems for drug delivery.

Introduction

Boron cluster compounds are boron-rich molecules of polyhedral geometry with the majority of vertices consisting of B–H units. Metallacarboranes, like cobalt bis(dicarbollide) anion, $[CoD]^-$, (see Scheme 1A) belong to this family, and they are extensively studied due to their stability and interesting properties.[1–4] They are considered as hydrophobic but water-soluble anions. It was demonstrated that they provide an unusual interaction potential resulting in self-assembly in solution[5,6] and complexation with various nanosystems.[7–25] They are utilized, for example, for ion extraction[26] and recently also in medicinal chemistry.[27–38] As regards medical applications, our interest is targeted to the preparation of stimuli-responsive hybrid nanosystems consisting of a nano-organized polymer matrix with embedded metallacarborane clusters,[39–42] which would lead to biocompatible vessels for drug-delivery purposes.[43–52] The importance of boron clusters is strengthened by the fact that some of their exoskeletal derivatives exhibit inhibition activity against enzymes like HIV protease and carbonic anhydrase.[31,38] After conjugation with biologically active molecules like nucleosides, DNA and cholesterol,[30,53–55] they can also act as their carriers.

Recently, we described the first type of unique nanostructures based on the complexation of hydrophilic poly(ethylene oxide), PEO, with water-soluble Na[CoD] resulting in an insoluble nanocomposite.[39] This phenomenon can be used for the preparation of micelles with PEO block in the core.[39,40] The main driving force for $[CoD]^-$ complexation with polymers is dihydrogen bonding of the slightly hydridic B–H vertices with the ethylene subunits of the PEO chain and with polymers consisting of a similar motif such as poly(2-alkyloxazolines), POX. However, the POX/metallacarborane complex is water soluble while the POE-complex is not.[41,42] The reason is that the Na^+ cation is not complexed by the amidic moiety in POX, but it interacts with oxy-groups in the case of PEO.[11,12] It was also reported that PEO/metallacarborane nanocomposite precipitation is significantly less pronounced in LiCl solution than it is in NaCl and KCl.[39] Further, we found that the short PEO linker spanning two metallacarborane clusters has an impact on their solution behavior because the cations can bind on the linker and other places of the molecule.[56] It is known that PEO chains form helical structures stabilized by the complexed cations, where K^+ has the highest affinity.[57] Furthermore, it was reported that interaction of cations with the amidic group is also selective.[58–60] This indicates that both POE and POX segments have a propensity to exhibit cation selectivity.

The above mentioned results initiated our deeper interest on the cation sensitivity of polymer/metallacarborane complexes.

[a]*Department of Physical and Macromolecular Chemistry, Faculty of Science, Charles University, Hlavova 2030, 128 40 Prague 2, Czech Republic. E-mail: pavel.matejicek@natur.cuni.cz; Fax: +420 224919752; Tel: +420 221951292*

[b]*Department of Applied Physics Nanotalo, Aalto University, Puumiehenkuja 2, FI-02150 Espoo, Finland*

[c]*Institute of Macromolecular Chemistry, v.v.i., Academy of Sciences of the Czech Republic, Heyrovský Sq. 2, 16206 Prague 6, Czech Republic*

[d]*Joint Institute for Nuclear Research, Dubna 141980, Moscow Region, Russia*

[e]*Taras Shevchenko National University of Kyiv, UA-01033 Kyev, Ukraine*

† Electronic supplementary information (ESI) available: Additional cryoTEM, light scattering and SANS results. See DOI: 10.1039/c5ra27588a

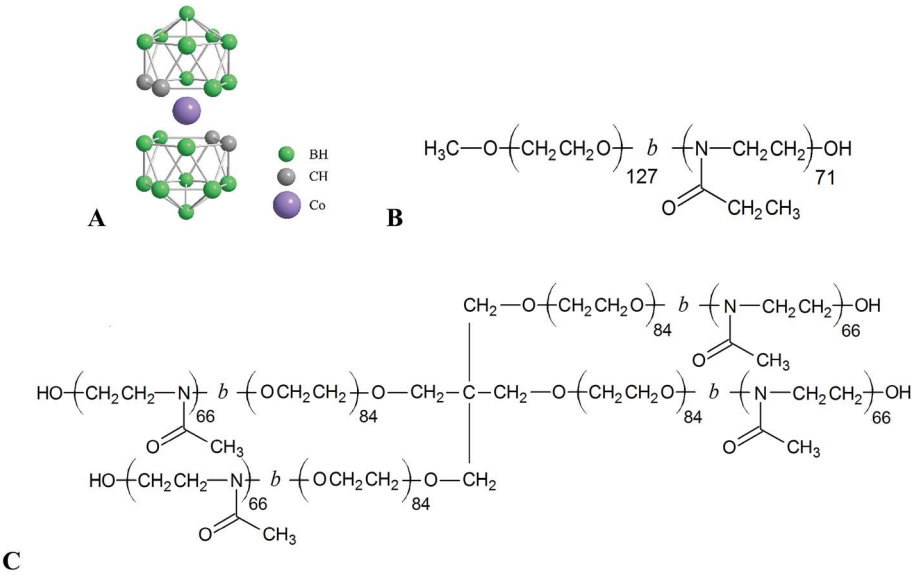

Scheme 1 Structures of (A) 3-cobalt bis(1,2-dicarbollide) and (B) double-hydrophilic block copolymer poly(ethylene oxide)-*block*-poly(2-ethyloxazoline) (PEO–POX) and (C) 4-arm poly(ethylene oxide)-*block*-poly(2-methyloxazoline), $[PEO–POX]_4$.

In this communication, our aim is to prepare polymeric nanostructures capable of exchanging bio-active metallacarboranes and cations. We used biocompatible and double-hydrophilic linear block copolymer poly(ethylene oxide)-*block*-poly(2-ethyloxazoline), PEO–POX (see Scheme 1B), and star-like block copolymer [poly(ethylene oxide)-*block*-poly(2-methyloxazoline)]$_4$, $[PEO–POX]_4$ (see Scheme 1C) as in our previous reports.[40,41] We used cryoTEM imaging and NMR spectroscopy in order to reveal the impact of alkaline cations on the compartmentalization within the hybrid nanoparticles. Isothermal titration calorimetry, ITC, was found to be a suitable method for monitoring of cation and metallacarborane exchange after an external stimulus was applied (addition of cation).

Compartmentalization in polymeric nanosystems and the controlled formation of hierarchically organized nanostructures currently belongs to the extensively studied field of macromolecular nanochemistry.[61–76] The formation of distinct compartments is usually induced by a hydrophobic effect and a non-compatibility of the building blocks.[61] Temperature and electrochemical processes also act as stimuli leading to the formation of nanostructures.[75,76] Another possibility is the co-assembly of polymers with low molecular mass compounds.[69,70]

Self- and co-assembly induced by inorganic salts have been studied mainly for the preparation of quantum dots (such as those formed by cadmium or lanthanides),[77,78] ferrofluids,[79] or for the delivery of metals like cisplatin for biomedical applications[80–82] and for the extraction of mercury.[83] Controlled drug release was described for hybrid polymer/silica nanoparticles after exchange of Zn^{2+} by H^+ ions.[84] Ion-sensitive resins (both cationic and anionic) and other polymers sensitive to external stimuli (temperature, hydration, salting-out effect, *etc.*) are used for counterion-responsive drug release during digestion in the human body.[81]

As concerns the controlled release of physiologically active LiCl, there are two approaches in the literature: polyelectrolyte hydrogels (*e.g.*, based on amino acid residues)[82] and current-controlled drug release from PEO-based electrolytes containing LiCl *via* iontophoresis.[85] Our system based on PEO–POX/metallacarborane nanoparticles can be thus considered as a third way for the delivery of alkaline cations with benefits such as the presence of bio-active boron cluster compounds.

Materials and methods

Materials

Metallacarborane cesium [3-cobalt bis(1,2-dicarbollide)]$^-$, Cs[CoD], was purchased from Katchem (Prague, Czech Republic). Poly(ethylene oxide)-*block*-poly(2-ethyloxazoline), PEO–POX, linear diblock copolymer and [poly(ethylene oxide)-*block*-poly(2-methyloxazoline)]$_4$, $[PEO–POX]_4$, star-like (4-arm) diblock copolymer were purchased from Polymer source, Inc. (Dorval, Quebec, Canada). The weight averaged relative molecular weight of the PEO and the POX blocks, as obtained by SEC and NMR,[42] are 5.6×10^3 and 7.0×10^3, $Đ = 1.8$ for PEO–POX, and 3.7×10^3 and 5.6×10^3, $Đ = 1.5$ for $[PEO–POX]_4$, respectively.

Preparation of Na[CoD], Li[CoD] and K[CoD]

The cationic exchange resin (Amberlite IR120, H form) was purchased from Acros Organics. Cs[CoD] was converted to Na[CoD], Li[CoD] and K[CoD] according to the following procedure: first, we charged the resin by passing 250 mL of 3 M HCl followed by rinsing with water. The column was loaded with lithium (or potassium respectively) cations by passing 3 M MCl preparation of M[CoD] (M = Li, Na and K) solution through resin, and then rinsing with around 500 mL of water (the eluent was tested to see if it contains traces of MCl by $AgNO_3$ solution). Solid Cs[CoD] was dissolved in a mixture of acetonitrile/water

(50 : 50) and this solution (around 100 mL) was passed repeatedly through (drop by drop) a cation exchanging resin loaded with the desired cation. The solvent was finally evaporated and the crude product was left to dry in a desiccator overnight. The water content in M[CoD] for M = Na, Li, K was determined by TGA to be 16%, 13%, and 0% (w/w), respectively.

Sample preparation

Samples of PEO–POX copolymers with M[CoD] in 0.154 M MCl (M stands for Na, Li and K) for light scattering, NMR, SANS and cryoTEM analysis were prepared as follows: the copolymer was dissolved in 0.154 M MCl. Stock aqueous solution of M[CoD] (0.0245 M) in 0.154 M MCl or solid M[CoD] was added to the polymer solution in the desired metallacarborane-to-polymer segment ratio, ξ. For NMR measurements, a small amount of *t*-butyl alcohol (1 μL) was added to the solution as an internal standard. A sample of PEO–POX/Li[CoD] (polymer concentration 10 g L^{-1}, $\xi = 0.045$) in 0.154 M LiCl was used for ITC and NMR titrations, where the nanoparticle dispersion was titrated by 0.154 M LiCl, NaCl and KCl solution.

Methods

Dynamic light scattering (DLS) and static light scattering (SLS). The light scattering setup (ALV, Langen, Germany) consisted of a 633 nm He–Ne laser, an ALV CGS/8F goniometer, an ALV High QE APD detector, and an ALV 5000/EPP multibit, multitau autocorrelator. DLS data analysis was performed by fitting the measured normalized intensity autocorrelation function $g_2(t) = 1 + \beta|g_1(t)|^2$, where $g_1(t)$ is the electric field correlation function, t is the lag-time and β is a factor accounting for deviation from the ideal correlation. An inverse Laplace transform of $g_1(t)$ with the aid of a constrained regularization algorithm (CONTIN) provides the distribution of relaxation times, $\tau A(\tau)$. Effective angle- and concentration-dependent hydrodynamic radii, $R_H(q, c)$, were obtained from the mean values of relaxation times, $\tau_m(q, c)$, of individual diffusive modes using the Stokes–Einstein equation. To obtain true hydrodynamic radii, the data have to be extrapolated to a zero scattering angle. Since the refractive index increment, d*n*/d*c*, is unknown for almost all of the samples, we evaluated in such cases only the light scattering intensity extrapolated to zero scattering angle as the measure proportional to molar mass of polymeric nanoparticles.

Cryo-transmission electron microscopy (cryo-TEM). Glow discharge (Emitech KX100, 2 min/25 mA) treated Quantifoil R2/2 holey carbon copper grid with a hole size of 2 μm was transferred into the environmental chamber of an FEI Vitrobot at room temperature and 100% humidity. 3 μL of sample solution was applied on the grid which was blotted for 1.5 seconds and then shot to a 1/1 mixture of liquid ethane and propane of temperature −180 °C. The grid with vitrified sample film was cryotransferred into a FEI Tecnai 12 transmission electron microscope with a Gatan 910 cryotransfer holder at a temperature of *ca.* −185 °C. Bright-field TEM was performed using an acceleration voltage of 120 kV and images were recorded on a Gatan Ultrascan 1000 CCD camera.

Small angle neutron scattering (SANS). The neutron experiments were performed using a YuMO spectrometer in the two detectors system mode. The beam was collimated to a diameter of 14 mm on the sample. The obtained spectra were put on the absolute intensity scale using a vanadium scatterer. Spectra were normalized by the standard procedure using SAS software.

^{1}H NMR spectroscopy. ^{1}H NMR spectra were measured on a Varian ^{UNITY}INOVA 400 in deuterium oxide (99.5%; Chemotrade, Leipzig, Germany). Spectra were referenced to the solvent signal (4.80 ppm).

Isothermal titration calorimetry (ITC). ITC measurements were performed with an Isothermal Titration Calorimeter (Nano ITC), TA Instruments – Waters LLC, New Castle, USA. The microcalorimeter consists of a reference cell and a sample cell (24K Gold). The sample cell is connected to a 50 μL syringe. The syringe needle is equipped with a flattened, twisted paddle at the tip, which ensures continuous mixing of the solutions in the cell rotating at 250 rpm. Titrations were carried out by consecutive 2 μL injections of a total 50 μL of 154 mM NaCl, LiCl and KCl from the syringe into the sample cell filled with 200 μL of 10 g L^{-1} PEO–POX/Li[CoD] in 154 mM LiCl and 154 mM LiCl for comparison. All titrations were doubled, thus a total of 50 injections were performed with an interval of 300 s. By this method then the differential heat of mixing is determined for discrete changes of composition.

Results and discussion

Structure of PEO–POX/metallacarborane nanoparticles in LiCl, NaCl and KCl

In our previous work, we already described several polymeric nanosystems based on mutual interaction of hydrophilic polymers with metallacarboranes like sodium cobalt bis(dicarbollide), Na[CoD], all of them exhibiting a unique inner structure:[11,12,39–42] diblock copolymers with one block not interacting with $[CoD]^-$ but the second one (PEO-block) forming an insoluble complex with $[CoD]^-$ form micelles with PEO-block in the micellar core. The metallacarboranes and their bio-active conjugates are embedded within the PEO-matrix and can be released upon external stimulus (NaCl concentration).[39,40] A situation, where both blocks interact with boron clusters (PEO and POX block copolymers),[41,42] also leads to stable nanoparticles capable of accumulating fairly large portions of metallacarborane-based inhibitors of HIV protease.[41] Among the roles of the copolymer architecture,[42] there is however another possibility to control the particle nanostructure and the release of active species: a proper selection of salt medium, an interesting phenomenon that has never been explored in detail before. In order to reveal the cation sensitivity of the polymer/metallacarborane nanoparticles, we prepared hybrid metallacarborane-containing nanoparticles from double-hydrophilic diblock copolymer PEO–POX and 4-arm diblock copolymer $[PEO–POX]_4$ (see Scheme 1) by consecutive addition of Li[CoD], Na[CoD] or K[CoD] in 0.154 M (physiological solution) LiCl, NaCl or KCl solutions, respectively.

The morphology of PEO–POX/M[CoD] in MCl (M = Na, Li, and K) nanoparticles was visualized by cryoTEM imaging

(shown in Fig. 1). Micrographs for the corresponding 4-arm systems, $[PEO–POX]_4$/M[CoD] in MCl (M = Na, Li, and K), are shown in Fig. S1 in the ESI.† A distinct compartmentalization in the Li- and K-media, and a formation of homogeneous nanospheres in the Na-medium for the PEO–POX linear diblock directly proves the impact of cations on the metallacarborane/polymer interaction. The particles are fairly polydisperse in general (kinetically controlled)[39] and there is a fraction of "small particles" that could be attributed to metallacarborane self-assemblies[5] and small pre-aggregates.[41] However, we will discuss the cation-selectivity on the structure of large particles exhibiting compartmentalization.

Long straight cylinders were detected in the K-system (see Fig. 1C). Such extended structures have never been observed for metallacarborane/polymer complexes before. The cylinders are longer than the contour length of single polymer chains, and their width is about 5 nm, which is close to dimensions of a single metallacarborane "micelle" (*ca.* 2.5 nm). Furthermore, some of them are shaped like a necklace of small spheres. The structure and origin of this shape is not clear yet, especially their straight shape. Our hypothesis is that it is closely related to the formation of extended helical structures of PEO–POX that are stabilized by complexation with K^+.[57]

The basic characterization of PEO–POX/M[CoD] in MCl nanoparticles was carried out by means of standard scattering techniques (light scattering and SANS). The results, which are in agreement with cryoTEM and previously reported data,[41,42] are provided in the ESI (Fig. S2 and 3 and Table S1†).

Size of the compartments

The cryoTEM micrographs were analyzed by means of ImageJ software in order to obtain size distributions of the large compact nanoparticles and especially compartments within them (see histograms in Fig. 1; results are summarized in Table 1). From the analysis, we found that compartments are slightly smaller in the Li-medium (diameter 3.8 ± 1.1 nm) than in the K-one (diameter 4.7 ± 1.3 nm). Further, the compartments are significantly larger than metallacarborane "micelles" (diameter 2.5 ± 0.7 nm).[5] As concerns the star-like copolymer, the diameter of the compartments is independent of the nature of cation (it is around 3.5 nm in all three cases). However, the interpretation of cryoTEM micrographs on a molecular level requires information on what kind of polymer segments (PEO or POX) are involved in the compartmentalization. This information would shed the light on the impact of cations on the metallacarborane polymer interaction. As shown below, NMR spectroscopy is a suitable tool for such a purpose.[39–42]

Structure of the compartments and their origin

We used the ^{1}H NMR technique to estimate the fraction of polymer segments involved in the complexation with M[CoD].

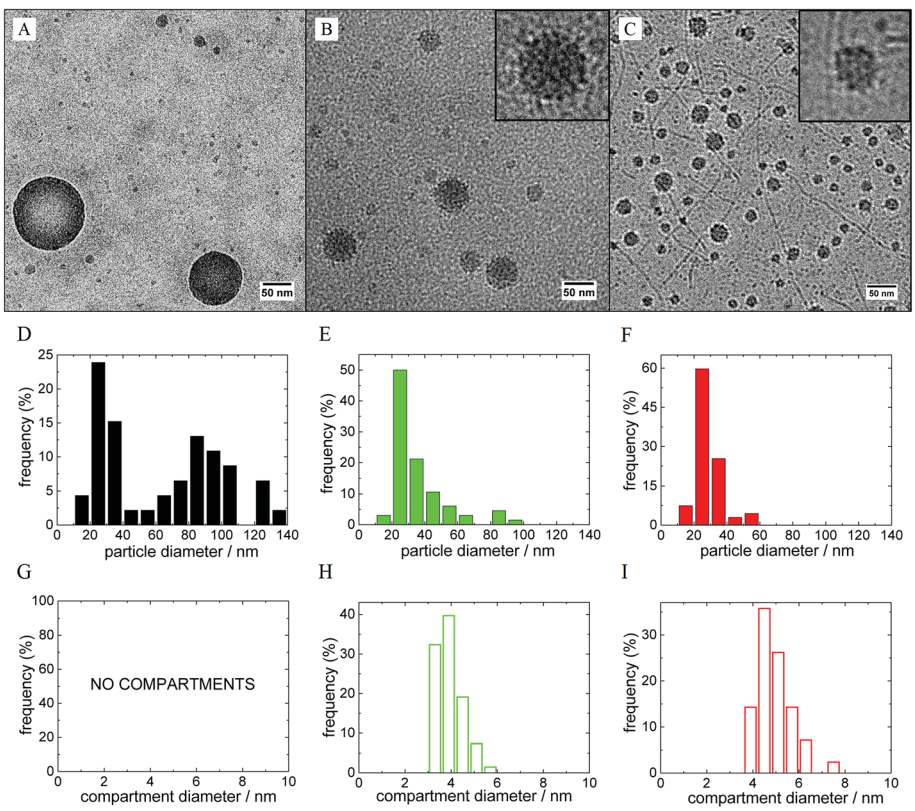

Fig. 1 CryoTEM micrographs of (A) PEO–POX/Na[CoD] in 0.154 M NaCl; (B) PEO–POX/Li[CoD] in 0.154 M LiCl; (C) PEO–POX/K[CoD] in 0.154 M KCl (polymer concentration 10 g L^{-1}). (D–I) Histograms based on the size analysis of nanostructures in different salt media (NaCl – black, LiCl – green, and KCl – red), where (D–F; filled columns) correspond to diameter distributions of "large" nanoparticles and (G–I; hollow columns) to diameter distributions of compartments within the "large" nanoparticles.

Table 1 Diameter of polymer/M[CoD] (M = Na, Li and K) nanoparticles and compartments within them from the analysis of the corresponding cryoTEM micrographs

	Particle diameter/nm		
	Medium		
	Sodium	Lithium	Potassium
Linear diblock PEO–POX			
Large particles	93.5	12	18.5
Compartments	NO	3.8 ± 1.1	4.7 ± 1.3
Compartments after ITC[a]	3.1 ± 0.8	4.2 ± 1.0	3.5 ± 0.9
Star-like [PEO–POX]$_4$			
Large particles	26.3	17.6	12.4
Compartments	3.4 ± 0.8	3.7 ± 1.4	3.4 ± 1.4

[a] Originally PEO–POX/Li[CoD] in 0.154 M LiCl sample, which was titrated by 0.154 M NaCl, LiCl and KCl solutions in the ITC experiment.

The fraction of frozen segments within the complex was calculated from the diminishing of the corresponding signals in NMR spectra as a function of ξ. The ratios of integrated intensities of ^{1}H signals of ethylene subunits in PEO and POX blocks to those in a molecularly dissolved polymer of the same concentration, which give the fractions of kinetically frozen monomer units, are shown in Fig. 2. In NaCl solution, the fraction of frozen POX is comparable to that of PEO, in the case of linear diblock (Fig. 2A). In LiCl solution, the fraction of frozen POX is much higher than that of PEO. An opposite effect occurs in the case of KCl solution, where PEO segments are substantially frozen as compared to POX. With respect to the cryoTEM analysis, it indicates that there is no preference of $[CoD]^-$ in the Na-medium towards PEO and POX segments resulting in homogeneous nanoparticles.[41] Interaction of $[CoD]^-$ with POX segments is preferred in the Li-medium, and POX blocks thus form compartments. Finally, K^+ ions support interaction of $[CoD]^-$ with PEO segments, and PEO blocks are forming the compartments in this case. Since the PEO block is almost twice as long (127 segments) as the POX one (71 segments), see Scheme 1B, we assume a different size of the PEO- and POX-compartments. This is in agreement with cryoTEM analysis (see Table 1), where compartments have dimensions 3.8 nm and 4.7 in lithium and potassium solutions, respectively.

The cation selectivity of PEO and POX segments towards $[CoD]^-$ can be explained with the help of literature data on cation interaction with species consisting of an amidic moiety (as it is also in POX).[58,59] It is also related to salting in and salting out effects of ions on PEO-like polymers with connotations to the famous Hofmeister series.[60] It was reported that Li^+ ion has higher affinity towards O-group in amidic compounds than Na^+,[58] and K^+ has high affinity towards PEO-chains forming stable helical structures.[57] Further, the PEO/metallacarborane precipitation is more pronounced in the Na- and K-medium than in the Li-one.[39]

Based on the above mentioned results, we assume the following scenario for cation-sensitive compartmentalization on the molecular level. It is known from calorimetry experiments that the $[CoD]^-$ cluster has roughly the same affinity towards PEO and POX segments in the Na-medium.[42] It should result in the formation of homogeneous nanostructures because none of the segments is preferred (see Fig. 1A). Na^+ counterions are tightly complexed by PEO units[11,12] but only slightly by POX units. This stabilizes the nanospheres in the form of a nanogel because of the uncompensated charge on POX/metallacarborane segments.[42] In the Li-medium, Li^+ counterions have high affinity towards POX segments, and $[CoD]^-$ only weakly binds to PEO segments.[39] This shifts the equilibrium towards the complexation of metallacarborane with POX blocks. In the K-medium, the situation is just the opposite. K^+ counterions are strongly bound by PEO-segments,[57] and PEO compartments are thus formed. In general, this confirms our general observations that the "solubility" of the otherwise hydrophobic $[CoD]^-$ anion is controlled by the mobility of counterions. If they are immobilized for any reason this leads to the formation of compact nanostructures like compartments. If the counterions remain free and the metallacarborane cluster is bound by the polymer, it results in gel-like structures.

Polymer architecture beats ion selectivity

Regarding the morphology of nanoparticles consisting of the star-like copolymer, the compartmentalization is observed in all

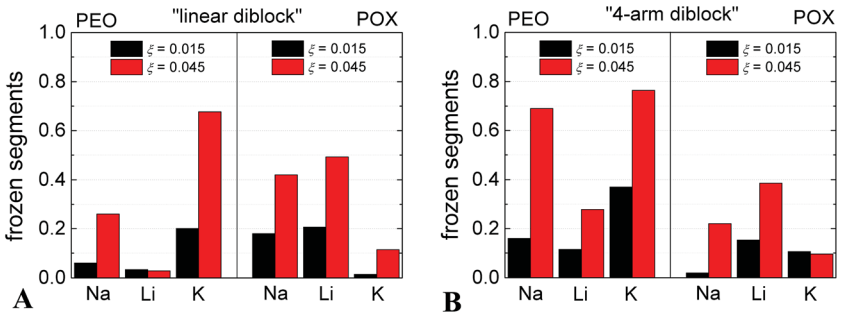

Fig. 2 Fraction of frozen polymeric segments in (A) PEO–POX/M[CoD] in MCl and (B) [PEO–POX]$_4$/M[CoD] in MCl (M = Na, Li and K) differing in M[CoD] content in 0.154 M MCl calculated from the decrease of the corresponding ^{1}H NMR signals relating to pure block copolymer and *t*-butanol (internal standard).

three media (Na, Li and K) (see micrographs in Fig. S1 in ESI† and their analysis in Table 1), and the compartments are of similar dimensions in all three cases. It is evident from NMR results (see Fig. 2B) that the star-like architecture with PEO blocks in the "core" of the star induced preferential compartmentalization of PEO segments[42] almost regardless of the cation type.

Cation selectivity of the nanoparticles: preferential sorption of Na^+ in Li-rich medium

In experiments dealing with the nanoparticles with a mix of alkaline cations, Na[CoD] was used instead of Li(K)[CoD] for the nanoparticle preparation in the Li(K)-medium. We noticed that the size of compartments in cryoTEM micrographs as well as the fraction of frozen segments from the NMR spectra is different as compared with systems in the entirely Li(K)-medium. This suggests that Na^+ is preferentially adsorbed within the nanoparticles in the otherwise Li-rich solution and even a low portion of Na^+ is enough to provoke changes in the nanoparticle inner structure. In the case of Na[CoD] in the K-medium, the effect of preferential Na^+ sorption is however fairly weak. For further details and experimental data see Fig. S4 and the corresponding part of the ESI.†

Cation exchange and its impact on the structure of nanoparticles

It encouraged us to study the ion-exchange issue in detail. We carried out isothermal titration calorimetry (ITC) experiments, where dispersion of PEO–POX/Li[CoD] nanoparticles in 0.154 M LiCl was titrated with 0.154 M LiCl, NaCl, and KCl solution. In Fig. 3A, there are raw heat rates. Since all the solutions have the same salt concentration (0.154 M), additional heats of dilution are negligible and do not interfere with cation exchange/sorption reactions. An almost zero heat flow is seen in the "Li to Li" experiment (green curves in Fig. 3A and B). However, the addition of NaCl and KCl (black and red curves, respectively) provokes two processes. They can be clearly distinguished in the zooms of the raw heat flow curves.[86–89] In the beginning of the titration, there is only one strongly exothermic process, which is related to the cation exchange or sorption. Close to the saturation, the endotherm of simple salt mixing appears which eventually prevails. The endothermic peak is sharp and occurs immediately after the injection. On the contrary, the ion exchange/sorption (related to the exotherm) is a relatively slow process, because it is accompanied by a mass flow (bulky metallacarborane clusters) and changes in the polymer chain conformation.

The heats of the ionic exchange ($\Delta H^{exchange}$) estimated as the intercept of the ITC curve with the *y*-axis (Fig. 3B) for "Na to Li" and "K to Li" processes are -6 kJ mol^{-1} and -16 kJ mol^{-1}, respectively. The heats are smaller than for the overall interaction of Na[CoD] with PEO/POX-polymers (around -40 kJ mol^{-1}),[11,41,42] but much larger than for the cation exchange of the relatively small "dumbbell" molecules (sub -1 kJ mol^{-1}).[56]

The shape of the ITC curves (Fig. 3B) is hardly comparable with a simple one-site binding model with a sigmoidal shape.[11,12] The shape without a plateau in the early stages of the titration indicates that there is not a single set of identical binding sites and that the inner structure of the nanoparticles is changing continually with increasing concentration of the guest cation.[86] This is why the value of ΔH^{obs} has to be estimated from the intercept with the *y*-axes rather than with fitting by a sigmoidal curve, which has no physical meaning in this case. However, the ITC curves are comparable with a partition model employed for example for distribution of small molecules in systems exhibiting a microphase separation.[87–89]

The saturation of the Li-based nanoparticles by K^+ and Na^+ occurred at molar ratios of 0.23 and 0.51, respectively (see leveling off of the red and black curves in Fig. 3B). To interpret this, we analyzed the structure changes during the titration also by cryoTEM and NMR (shown as Fig. S5 with further comments in the ESI†). It is evident that the addition of K^+ leads to the "melting" of POX compartments and formation of PEO ones. K-ions bind only to a limited portion of polymer segments (*ca.* 25%) most likely to PEO blocks. Saturation of the nanoparticles by Na^+ requires a higher portion of the cation (*ca.* 50% of both POE and POX segments) accompanied by diminishing of the compartments. The overall fraction of the frozen segments remains however roughly the same. From the above mentioned results, it seems that metallacarborane clusters are rapidly released from POX-domains and migrate towards PEO-rich areas after addition of KCl to the Li-medium. The changes after addition of NaCl are milder and slower than the previous

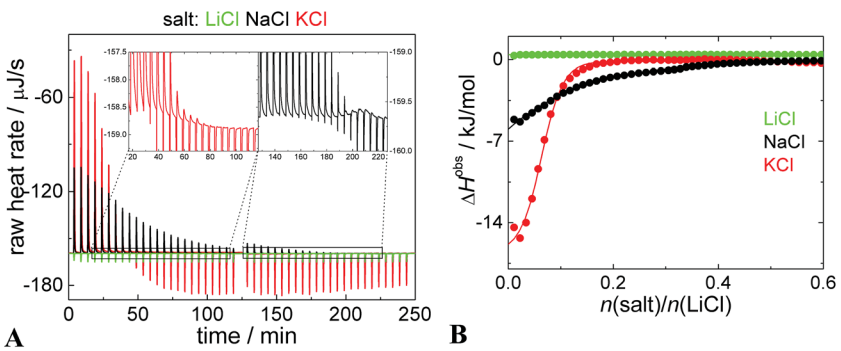

Fig. 3 (A) ITC raw heat flows including zooms and (B) corresponding thermograms with subtracted heats of mixing (dilution) for 0.154 M NaCl, LiCl and KCl titrated into 0.154 M LiCl solution of PEO–POX/Li[CoD] particles with $\xi = 0.301$ (the polymer segment-to-Li^+ ratio is around 1 : 1).

ones, and the compartments partly homogenize within the nanoparticles.

Conclusions

Mono-anionic metallacarboranes like cobalt bis(dicarbollides), $[CoD]^-$, which are fully artificial boron cluster compounds with unusual binding capacity and interesting bio-activity, interact with water soluble polymers like poly(ethylene oxide), PEO, and poly(2-alkyloxazoline), POX, *via* dihydrogen bonding between B–H vertices and C–H groups of the polymeric backbone. The affinity of the anionic cluster to both PEO and POX segments is roughly the same, but the key-factor affecting the compact complex formation is the selectivity of alkaline cations towards PEO and POX segments. This is a phenomenon that has never been studied in detail before.

In the Na-medium, there is no preference and homogeneous nanospheres with $[CoD]^-$ bound to both types of segments are formed. In the Li-medium, interaction of both Li^+ and $[CoD]^-$ with POX segments is preferred resulting in distinct compartmentalization of POX segments within the hybrid nanoparticles. In the K-medium, the situation is just the opposite and PEO-compartments are formed instead. The PEO–POX/M[CoD] in MCl (M = Li, Na and K) nanoparticles and compartments within them were studied by means of cryoTEM imaging, NMR spectroscopy and ITC calorimetry.

An exchange of cations of different affinity was demonstrated by titrations with NaCl, KCl and LiCl solutions monitored by ITC, cryoTEM and NMR. It is clear that even a small amount of K^+ and Na^+ ions provokes substantial changes in the inner structure of the nanoparticles accompanied by the flux of metallacarborane clusters and alkaline cations. This is the first example, where compartmentalization in polymeric nanoparticles is controlled by the selectivity of alkaline cations. With respect to bio-activity of metallacarborane clusters and also alkaline cations like Li^+, the nanoparticles can be utilized for stimuli-responsive drug delivery.

Acknowledgements

The authors would like to acknowledge financial support of Czech Science Foundation P205/14-14608S and P106/12/0143, and The Charles University Grant Agency GAUK 512214. The authors thank Adnana Zaulet, Clara Vinas and Francesc Teixidor (ICMAB, Barcelona) for the preparation of potassium and lithium salts of cobalt bis(dicarbollide).

References

1 R. N. Grimes, *Coord. Chem. Rev.*, 2000, **200**, 773.
2 J. Plesek, *Chem. Rev.*, 1992, **92**, 269.
3 I. B. Sivaev and V. I. Bregadze, *Collect. Czech. Chem. Commun.*, 1999, **64**, 783.
4 P. Farras, E. J. Juarez-Perez, M. Lepsik, R. Luque, R. Nunez and F. Teixidor, *Chem. Soc. Rev.*, 2012, **41**, 3445.
5 M. Uchman, V. Dordovic, Z. Tosner and P. Matejicek, *Angew. Chem., Int. Ed.*, 2015, **54**, 14113.
6 P. Bauduin, S. Prevost, P. Farras, F. Teixidor, O. Diat and T. Zemb, *Angew. Chem., Int. Ed.*, 2011, **50**, 5298.
7 R. N. Grimes, *Dalton Trans.*, 2015, **44**, 5939.
8 M. Uchman, P. Jurkiewicz, P. Cigler, B. Gruner, M. Hof, K. Prochazka and P. Matejicek, *Langmuir*, 2010, **26**, 6268.
9 K. Kowalski, T. Goszczynski, Z. J. Lesnikowski and J. Boratynski, *ChemBioChem*, 2015, **16**, 424.
10 M. Tarres, E. Canetta, E. Paul, J. Forbes, K. Azzouni, C. Vinas, F. Teixidor and A. J. Harwood, *Sci. Rep.*, 2015, **5**, 7804.
11 P. Matejicek, J. Brus, A. Jigounov, J. Plestil, M. Uchman, K. Prochazka and M. Gradzielski, *Macromolecules*, 2011, **44**, 3847.
12 J. Brus, A. Zhigunov, J. Czernek, L. Kobera, M. Uchman and P. Matejicek, *Macromolecules*, 2014, **47**, 6343.
13 J. Rak, M. Jakubek, R. Kaplanek, P. Matejicek and V. Kral, *Eur. J. Med. Chem.*, 2011, **46**, 1140.
14 C. Masalles, J. Llop, C. Vinas and F. Teixidor, *Adv. Mater.*, 2002, **14**, 826.
15 S. Gentil, E. Crespo, I. Rojo, A. Friang, C. Vinas, F. Teixidor, B. Gruner and D. Gabel, *Polymer*, 2005, **46**, 12218.
16 C. Masalles, S. Borros, C. Vinas and F. Teixidor, *Adv. Mater.*, 2000, **12**, 1199.
17 J. G. Planas, C. Vinas, F. Teixidor, A. Comas-Vives, G. Ujaque, A. Lledos, M. E. Light and M. B. Hursthouse, *J. Am. Chem. Soc.*, 2005, **127**, 15976.
18 R. N. Grimes, *Mol. Cryst. Liq. Cryst.*, 2000, **342**, 7.
19 P. Farras, F. Teixidor, R. Kivekas, R. Sillanpaa, C. Vinas, B. Gruner and I. Cisarova, *Inorg. Chem.*, 2008, **47**, 9497.
20 E. J. Juarez-Perez, C. Vinas, F. Teixidor, R. Santillan, N. Farfan, A. Abreu, R. Yepez and R. Nunez, *Macromolecules*, 2010, **43**, 150.
21 B. P. Dash, R. Satapathy, J. A. Maguire and N. S. Hosmane, *Organometallics*, 2010, **29**, 5230.
22 J. G. Planas, F. Teixidor, C. Vinas, M. E. Light and M. B. Hursthouse, *Chem.–Eur. J.*, 2007, **13**, 2493.
23 E. J. Juarez-Perez, M. Granier, C. Vinas, H. Mutin and R. Nunez, *Chem.–Asian J.*, 2012, **7**, 277.
24 E. J. Juarez-Perez, H. Mutin, M. Granier, F. Teixidor and R. Nunez, *Langmuir*, 2010, **26**, 12185.
25 R. Nunez, E. J. Juarez Perez, F. Teixidor, R. Santillan, N. Farfan, A. Abreu, R. Yepez and C. Vinas, *Inorg. Chem.*, 2010, **49**, 9993.
26 B. Gruner, J. Plesek, J. Baca, I. Cisarova, J. F. Dozol, H. Rouquette, C. Vinas, P. Selucky and J. Rais, *New J. Chem.*, 2002, **26**, 1519.
27 I. B. Sivaev and V. V. Bregadze, *Eur. J. Inorg. Chem.*, 2009, **11**, 1433.
28 D. Gabel, *Pure Appl. Chem.*, 2015, **87**, 173.
29 M. Scholz and E. Hey-Hawkins, *Chem. Rev.*, 2011, **111**, 7035.
30 Z. J. Lesnikowski, *Collect. Czech. Chem. Commun.*, 2007, **72**, 1646.
31 P. Rezacova, P. Cigler, P. Matejicek, M. Lepsik, J. Pokorna, B. Gruner and J. Konvalinka, Medicinal Application of Carboranes: Inhibition of HIV Protease, in *Boron Science: New Technologies and Applications*, ed. N. S. Hosmane, CRC Press, New York, 2012, pp. 41–70.

32 R. F. Barth, A. H. Soloway, J. H. Goodman, R. A. Gahbauer, N. Gupta, T. E. Blue, W. L. Yang and W. Tjarks, *Neurosurgery*, 1999, **44**, 433.
33 A. H. Soloway, W. Tjarks, B. A. Barnum, F. G. Rong, R. F. Barth, I. M. Codogni and J. G. Wilson, *Chem. Rev.*, 1998, **98**, 1515.
34 M. F. Hawthorne, *Angew. Chem., Int. Ed.*, 1993, **32**, 950.
35 M. F. Hawthorne and A. Maderna, *Chem. Rev.*, 1999, **99**, 3421.
36 R. Satapathy, B. P. Dash, J. A. Maguire and N. S. Hosmane, *Collect. Czech. Chem. Commun.*, 2010, **75**, 995.
37 F. Issa, M. Kassiou and L. M. Rendina, *Chem. Rev.*, 2011, **111**, 5701.
38 J. Brynda, P. Mader, V. SIcha, M. Fabry, K. Poncova, M. Bakardiev, B. Gruner, P. Cigler and P. Rezacova, *Angew. Chem., Int. Ed.*, 2013, **52**, 13760.
39 P. Matejicek, J. Zednik, K. Uselova, J. Plestil, J. Fanfrlik, A. Nykanen, J. Ruokolainen, P. Hobza and K. Prochazka, *Macromolecules*, 2009, **42**, 4829.
40 M. Uchman, P. Cigler, B. Gruner, K. Prochazka and P. Matejicek, *J. Colloid Interface Sci.*, 2010, **348**, 129.
41 V. Dordovic, M. Uchman, K. Prochazka, A. Zhigunov, J. Plestil, A. Nykanen, J. Ruokolainen and P. Matejicek, *Macromolecules*, 2013, **46**, 6881.
42 V. Dordovic, M. Uchman, A. Zhigunov, A. Nykanen, J. Ruokolainen and P. Matejicek, *ACS MacroLett.*, 2014, **3**, 1151.
43 A. Wicki, D. Witzigmann, V. Balasubramanian and J. Huwyler, *J. Controlled Release*, 2015, **200**, 138.
44 J. A. MacKay, M. Chen, J. R. McDaniel, W. Liu, A. J. Simnick and A. Chilkoti, *Nat. Mater.*, 2009, **8**, 993.
45 R. Cheng, F. Feng, F. Meng, C. Deng, J. Feijen and Z. Y. Zhong, *J. Controlled Release*, 2011, **152**, 2.
46 R. J. R. Peters, M. Marguet, S. Marais, M. W. Fraaije, J. C. M. van Hest and S. Lecommandoux, *Angew. Chem., Int. Ed.*, 2014, **53**, 146.
47 T. C. Yih and M. Al-Fandi, *J. Cell. Biochem.*, 2006, **97**, 1184.
48 A. Harada and K. Kataoka, *Prog. Polym. Sci.*, 2006, **31**, 949.
49 Q. Zhao and P. H. Ni, *Prog. Chem.*, 2006, **18**, 768.
50 J. Rodriguez-Hernandez, F. Checot, Y. Gnanou and S. Lecommandoux, *Prog. Polym. Sci.*, 2005, **30**, 691.
51 E. S. Gil and S. A. Hudson, *Prog. Polym. Sci.*, 2004, **29**, 1173.
52 A. Lavasanifar, J. Samuel and G. S. Kwon, *Adv. Drug Delivery Rev.*, 2002, **54**, 169.
53 M. Matuszewski, A. Kiliszek, W. Rypniewski, Z. J. Lesnikowski and A. B. Olejniczak, *New J. Chem.*, 2015, **39**, 1202.
54 A. B. Olejniczak, J. Plesek, O. Kriz and Z. J. Lesnikowski, *Angew. Chem., Int. Ed.*, 2003, **42**, 5740.
55 M. Bialek-Pietras, A. B. Olejniczak, S. Tachikawa, H. Nakamura and Z. J. Lesnikowski, *Bioorg. Med. Chem.*, 2013, **21**, 1136.
56 M. Tarres, C. Vinas, P. Gonzalez-Cardoso, M. M. Hanninen, R. Sillanpaa, V. Dordovic, M. Uchman, F. Teixidor and P. Matejicek, *Chem.–Eur. J.*, 2014, **20**, 6786.
57 Y. Yokoyama, R. Hirajima, K. Morigaki, Y. Yamaguchi and K. Ueda, *J. Am. Soc. Mass Spectrom.*, 2007, **18**, 1914.
58 H. I. Okur, J. Kherb and P. S. Cremer, *J. Am. Chem. Soc.*, 2013, **135**, 5062.
59 C. Yan and T. Mu, *Phys. Chem. Chem. Phys.*, 2015, **17**, 3241.
60 J. C. Lutter, T. Y. Wu and Y. Zhang, *J. Phys. Chem. B*, 2013, **117**, 10132.
61 L. Zhang and A. Eisenberg, *Science*, 1995, **268**, 1728.
62 T. P. Lodge, A. Rasdal, Z. Li and M. A. Hillmyer, *J. Am. Chem. Soc.*, 2005, **127**, 17608.
63 J. F. Lutz and A. Laschewsky, *Macromol. Chem. Phys.*, 2005, **206**, 813.
64 Z. B. Li, M. A. Hillmyer and T. P. Lodge, *Macromolecules*, 2006, **39**, 765.
65 C. LoPresti, H. Lomas, M. Massignani, T. Smart and G. Battaglia, *J. Mater. Chem.*, 2009, **19**, 3576.
66 Z. B. Li, E. Kesselman, Y. Talmon, M. A. Hillmyer and T. P. Lodge, *Science*, 2004, **306**, 98.
67 R. C. Hayward and D. J. Pochan, *Macromolecules*, 2010, **43**, 3577.
68 S. Zhong, H. G. Cui, Z. Y. Chen, K. L. Wooley and D. J. Pochan, *Soft Matter*, 2008, **4**, 90.
69 M. Uchman, M. Gradzielski, B. Angelov, Z. Tosner, J. Oh, T. Chang, M. Stepanek and K. Prochazka, *Macromolecules*, 2013, **46**, 2172.
70 M. Uchman, S. Pispas, L. Kovacik and M. Stepanek, *Macromolecules*, 2014, **47**, 7081.
71 P. Matejicek, F. Uhlik, Z. Limpouchova, K. Prochazka, Z. Tuzar and S. E. Webber, *Macromolecules*, 2002, **35**, 9487.
72 F. Uhlik, Z. Limpouchova, P. Matejicek, K. Prochazka, Z. Tuzar and S. E. Webber, *Macromolecules*, 2002, **35**, 9497.
73 Y. A. Lin, Y. C. Ou, A. G. Cheetham and H. G. Cui, *ACS Macro Lett.*, 2013, **2**, 1088.
74 Z. B. Li, M. A. Hillmyer and T. P. Lodge, *Nano Lett.*, 2006, **6**, 1245.
75 F. A. Plamper, L. Murtomaki, A. Walther, K. Kontturi and H. Tenhu, *Macromolecules*, 2009, **42**, 7254.
76 F. Plamper, J. R. McKee, A. Laukkanen, A. Nykanen, A. Walther, J. Ruokolainen, V. Aeyev and H. Tenhu, *Soft Matter*, 2009, **5**, 1812.
77 M. Uchman, K. Prochazka, K. Gatsouli, S. Pispas and M. Spirkova, *Colloid Polym. Sci.*, 2011, **289**, 1045.
78 A. Sedlmeier and H. H. Gorris, *Chem. Soc. Rev.*, 2015, **44**, 1526.
79 R. Ladj, A. Bitar, M. M. Eissa, H. Fessi, Y. Mugnier, R. le Dantec and A. Elaissari, *Int. J. Pharm.*, 2013, **458**, 230.
80 B. Surnar, K. Sharma and M. Jayakannan, *Nanoscale*, 2015, **7**, 17964.
81 T. Yoshida, T. C. Lai, G. S. Kwon and K. Sako, *Expert Opin. Drug Delivery*, 2013, **10**, 1497.
82 M. Casolaro and I. Casolaro, *Polymers*, 2012, **4**, 964.
83 B. Hashemi, M. Shamsipur, A. Javadi, M. K. Rofouei, A. Shockravi, N. Tajarrod and N. Mandumy, *Anal. Methods*, 2015, **7**, 9641.
84 L. Xing, H. Zheng, Y. Cao and S. Che, *Adv. Mater.*, 2012, **24**, 6433.
85 T. S. Sahota, R. J. Latham, R. G. Linford and P. M. Taylor, *Drug Dev. Ind. Pharm.*, 2000, **26**, 1039.
86 O. Mertins and R. Dimova, *Langmuir*, 2011, **27**, 5506.

87 F. M. Coreta-Gomes, P. A. T. Martins, A. Velazquez-Campoy, W. L. C. Vaz, C. F. G. Geraldes and M. J. Moreno, *Langmuir*, 2015, **31**, 9097.

88 M. J. Moreno, M. Bastos and A. Velazquez-Campoy, *Anal. Biochem.*, 2010, **399**, 44.

89 H. Osanai, T. Ikehara, S. Miyauchi, K. Shimono, J. Tamogami, T. Nara and N. Kamo, *J. Biophys. Chem.*, 2013, **4**, 11.